Intramolecular structural model for photoinduced plasticity in chalcogenide glasses

S. N. Yannopoulos*
Foundation for Research and Technology Hellas, Institute of Chemical Engineering and High Temperature Chemical Processes (FORTH/ICE-HT), P.O. Box 1414, GR-26500, Patras, Greece
(Received 8 October 2002; revised manuscript received 20 March 2003; published 25 August 2003)

Selected spectral features of Raman spectra of glassy As_2S_3 subjected to elongation stress and sub-band-gap light illumination are analyzed and compared with polarization-dependent information obtained from the bulk glass at room temperature and near the glass transition temperature. The data are suggestive of specific structural changes which involve the transformation of atomic arrangements from realgarlike As_4S_4 molecules, originally present in virgin (untreated) fibers, into planar orpimentlike clusters. Implications of these atomic rearrangements to the incipient photoinduced fluidity—the onset of plastic deformation—in As_2S_3 glass are discussed. Kinetics of photoinduced plastic changes is compared to that of Raman spectra changes, revealing a qualitative similar behavior. An approximate estimation of the relative contribution of intermolecular rearrangements and the intramolecular structural mechanism proposed in this paper has revealed that the latter is responsible for almost 30% of the photoinduced elongation of the fiber's length at room temperature. The proposed mechanism can as well serve as rationale for understanding the photoinduced volume expansion observed in chalcogenide glasses.

DOI: 10.1103/PhysRevB.68.064206 PACS number(s): 63.50.+x, 42.70.Gi, 61.43.Dq, 78.30.−j

I. INTRODUCTION

Morphic effects, originating from changes in the short- and/or medium-range structures of materials, can be induced by means of external stimuli such as temperature and pressure. However, an interesting class of structural metamorphoses arises when an amorphous semiconductor and in particular a chalcogenide glass is illuminated with light having energy comparable to its band-gap energy; for general reviews on the subject see Refs. 1 and 2. The relatively recently reported photoinduced fluidity (PiF) is one of the most fascinating yet less studied photoplastic effects.[3] PiF pertains to the plastic deformation or permanent shape changes of a chalcogenide glass (manufactured in the form of a fiber or a flake) induced by light illumination in a purely athermal way. The athermal increase in a material's plasticity is achieved through the *combined* effect of sub-band-gap light illumination and the simultaneous application of external mechanical stress, as was demonstrated for the As_2S_3 glass.[3] Perhaps the most provocative feature of PiF is its anomalous temperature dependence, namely, the fact that PiF is hindered at higher temperatures.

The macroscopic changes observed (i.e., fiber elongation) imply that PiF is the cumulative effect of structural rearrangements occurring at the molecular level and hence Raman-scattering studies are appropriate for elucidating the microscopic origin of the effect. The study is simplified since a single light source is used to both induce and record the photostructural changes. This is accomplished by collecting the right-angle scattered light during optical processing of the stressed fiber. In addition, Raman scattering is able to probe both intermolecular and intramolecular vibrational modes,[4] thus furnishing valuable information concerning the short- and medium-range structures.[5] An extensive study concerning changes in intramolecular and intermolecular vibrational modes of As_2S_3 and the nonstoichiometric $As_{25}S_{75}$ composition in the athermal PiF regime has recently been undertaken by our group.[6–10] A synopsis of these works can be found elsewhere.[11]

As noticed elsewhere[3] the nature of PiF is purely photoelectronic and the atomic rearrangement might involve changes of either intramolecular (covalent, strong) and/or intermolecular (van der Waals, weak) bonds. However, intramolecular and intermolecular mechanisms cover actually any kind of structural mechanisms that can be envisaged and thus critical analysis of Raman-scattering studies can be proved useful for substantiating particular structural models. The purpose of the present paper is to propose an atomistic structural model for PiF which involves intramolecular atomic changes. The model suggested here is based on clear experimental evidence concerning the spectral properties of particular Raman peaks.

The paper is arranged as follows. In Sec. II a brief experimental description is presented. Section III A contains the results and their discussion in the context of existing data on the vibrational modes of As_4S_4 molecules. Based on the findings of this work an intramolecular structural mechanism compatible with the experimental data is proposed in Sec. III B. A qualitative comparison between the kinetics of photoinduced plastic changes with the time dependence of changes in the Raman spectra is attempted in Sec. III C. The contribution to fiber elongation of the proposed intramolecular structural model relative to that caused by other intermolecular mechanisms is estimated on a quantitative basis in Sec. III D. Finally, Sec. IV summarizes the conclusions drawn from the present study.

II. EXPERIMENT

The experimental procedure (fiber preparation and details about the light-scattering apparatus) have been described in detail elsewhere[7,9] and are thus only briefly mentioned here. As_2S_3 fibers were drawn from the melt at about 600 °C with slow drawing rates.[12] Fiber diameters, measured with the aid

of an optical microscope, where found to be in the range 100–280 μm. The fibers were attached to a stretching microdevice in a geometry perpendicular to the scattering plane. Bulk glasses were obtained by fast quenching the liquid which was previously kept at 600 °C for 3 h. The liquid and the obtained glass were contained in evacuated quartz tubes with dimensions 8 mm o.d.−6 mm i.d.

Stokes-side Raman spectra of fibers and the bulk glass were recorded with a conventional Raman spectrometer at a right angle. The excitation source was a Kr^+ laser (Spectra Physics) operating at 647.1 nm (1.92 eV) with low power density on the samples. The role of the power density is discussed in the next sections. Scattered light was analyzed by a double monochromator and recorded by a photomultiplier system equipped with standard electronics. The resolution used for all Raman measurements was $\sim$1.0 cm^{-1} in order to achieve high quality spectra. Accumulation times where chosen so as to obtain spectra of a high signal-to-noise ratio in order to facilitate the analysis of low intensity peaks. Both polarized (vertical polarization of incident laser–vertical analysis of scattered light, VV) and depolarized (horizontal polarization of incident laser–vertical analysis of scattered light, HV) were employed.

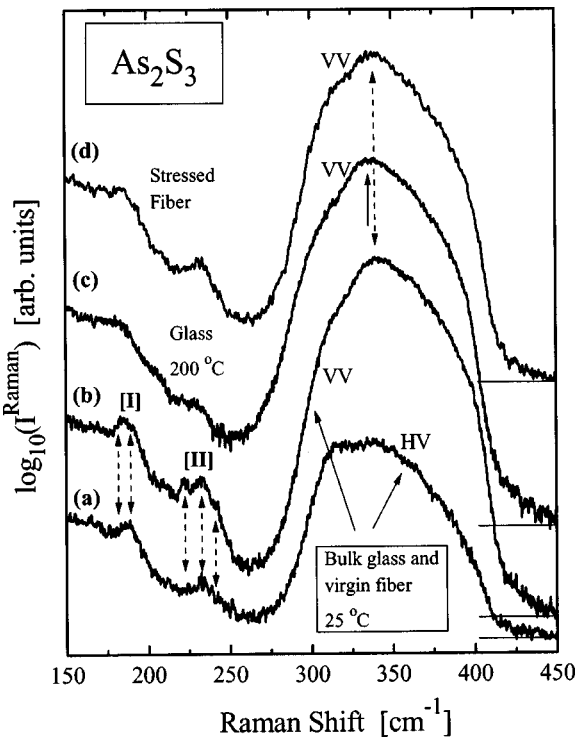

FIG. 1. Right-angle, Stokes-side Raman spectra of glassy As_2S_3. (a) and (b) Polarized (VV) and depolarized (HV) spectra of bulk glass at room temperature. (c) Polarized (VV) spectrum of bulk glass just below its glass transition temperature. (d) Polarized (VV) spectrum of an optically processed fiber. Note that intensities are shown in a logarithmic ($\log_{10}$) scale. Horizontal lines at the rightmost part of the figure denote the baselines of the spectra, which have been offset for clarity.

III. RESULTS AND DISCUSSION

A. Changes of the As_4S_4 molecule vibrational features under different external stimuli

In our previous studies on PiF, which included a room-temperature study of As_2S_3,[6,7] a temperature-dependence study of As_2S_3,[8,9] and a wavelength-dependence study of $As_{25}S_{75}$,[9] the main concern was the stress dependence of the polarization properties of scattered light. By means of the latter, ordering effects and the concomitant formation of anisotropic structures were monitored. However, the spectral properties of particular vibrational lines in the spectrum, and in particular their intensity dependence on external parameters, can also afford useful information that enables one to address the presence of certain ''chemical species'' or molecular units present in the glass structure. This is especially so because each of these species has a characteristic signature (frequency, polarization, etc.) in the Raman spectrum.

The curves in Figs. 1(a) and 1(b) illustrate high-frequency ($\nu > 150$ cm^{-1}) Raman spectra of polarized VV and depolarized HV As_2S_3 bulk glass at room temperature, respectively. The Raman spectra of the As_2S_3 bulk glass just below the glass transition temperature [Fig. 1(c)] and that of an optically processed fiber (with diameter $d \approx 250$ μm) of the same material [Fig. 1(d)] are also shown for comparison. The fiber has been subjected to a standard sub-band-gap light illumination and stretching procedure,[7,9] which involves a stepwise increase of elongational stress in which spectra were recorded at selected time intervals for different magnitudes of the applied stress. Illumination was held ''on'' continuously, even during time intervals between spectra recording. Since the spectra of the bulk glass and the virgin (as-drawn) fiber are practically identical we present in Fig. 1 only one of these data sets for clarity. Low-frequency modes, i.e., the features of the boson peak, have been the subject of previous studies[7,10,11] and are not discussed in the present paper.

As mentioned above, in previous studies we had almost exclusively focused on the polarization properties of scattered light. On the contrary, to extend the information that can be retrieved from the Raman spectra, in the present paper we pay attention to the intensity dependence of certain bands on external parameters such as temperature and stress. This analysis reveals information that can support a specific structural mechanism accounting for the still poorly understood microscopic nature of PiF. The mechanism suggested here emerges from clear experimental evidence, in contrast to a number of other structural models for photoinduced effects which are usually speculative. Being more specific, as one can deduce from the spectra reported in Fig. 1, the peaks located in regions I and II—which are fingerprints of the intramolecular (bond-bending) vibrational modes of As_4S_4 molecular units[13,14]—show noticeable changes in differently treated samples. Spectra in Figs. 1(a) and 1(b) show the polarization properties of these particular vibrational modes denoted by the dashed arrows. In region I we observe that the 182-cm^{-1} peak is strongly polarized while the 189-cm^{-1} peak is almost totally depolarized. Correspondingly, in spectral region II the vibrational modes located at 221 and 240 cm^{-1} are strongly polarized while the peak at 231 cm^{-1} is

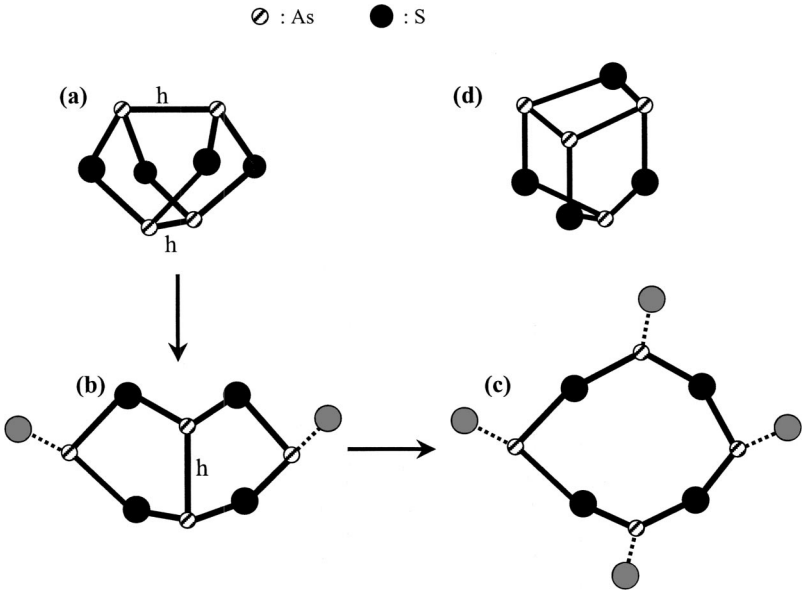

FIG. 2. A possible transformation of a locally planar morphogenesis [(a)→(b)→(c)]. The highly symmetrical (realgarlike) As_4S_4 molecule unfolds, giving rise to planar (orpimentlike) configurations. The homopolar or wrong As-As bonds are denoted by *h*. For details see text. (d) Schematic representation of the pararealgar (p-As_4S_4) molecular unit.

depolarized. These remarks are proved useful in the subsequent discussion in which the polarization properties and the frequencies of the vibrational modes of As_4S_4 in various environments are discussed.

Let us now proceed to the temperature dependence of the intensity of the aforementioned vibrational modes, when the As_2S_3 glass is heated at 200 °C (which is close to the glass transition temperature $T_g \approx 210$ °C), see Fig. 1(c). It is clearly seen that the intensity of the polarized band at 182 cm^{-1} is greatly reduced with increasing temperature while the depolarized peak at 189 cm^{-1} almost disappears, leading therefore to an almost flat depolarized spectrum in spectral region II (not shown in this figure for clarity). Similar drastic changes occur in region II, where the strongly polarized bands at 221- and 240-cm^{-1} peaks are not visible at 200 °C and the intensity of the depolarized 231-cm^{-1} band significantly diminishes. Interestingly, in the case of the optically processed fiber, i.e., at some stage of the PiF, the laser action selectively affects the two vibrational modes of regions I and II, the spectrum in Fig. 1(d). In region I the intensity of both peaks strongly diminishes. Finally, in region II the intensity changes during the photoplastic deformation are less drastic for the 231-cm^{-1} peak while at the same time the two polarized bands at 221 and 240 cm^{-1} are almost absent from the spectrum.

All the observations mentioned above imply that particular structural changes take place when changing the temperature or while subjecting the glass structure to the combined illumination/stretching process. Raman peaks are manifestations of the presence of different ''chemical species'' or molecular units, and hence from changes of peak intensities particular microscopic models can be verified or discarded. This, however, requires that at least some structural knowledge exists for the investigated system, and in this case diffraction studies are of paramount importance.

Before presenting a possible model suitable to account for the spectral changes mentioned above, some extra information on the vibrational properties of the As_4S_4 molecule [see Fig. 2(a) for a schematic representation of this molecule] should be given to facilitate the subsequent discussion. The presence, and especially the fraction, of homopolar As-As bonds in the stoichiometric glass are long-standing issues in studies of As chalcogenide glasses. It has been proposed that, even in the stoichiometric glass, above the melting point a fraction of the heteropolar As-S bonds dissociates, giving rise to homopolar As-As and S-S bonds through the endothermic reaction $2|\text{As-S}| \rightarrow |\text{As-As}| + |\text{S-S}|$.[15] With increasing temperature of the melt the fraction of the As-As bonds also increases. The homopolar or ''wrong'' bonds act as defects in the chemically ordered structure of the stoichiometric composition. Therefore, the fast quenching of the high-temperature liquid phase of As_2S_3 makes it possible to capture the chemically broken structure of the liquid into a metastable solid configuration. The homopolar bonds formed during this procedure remain stable given that the glass is not heated close to it glass transition temperature, where annealing effects will reestablish chemical order. Analyses of Raman spectra of As_2S_3 glass obtained by quenching the liquid from different temperatures have been interpreted as evidence for a 1% concentration of As-As bonds.[16] Since in our experiments we have prepared both the bulk glass and the fibers by fast cooling the high-temperature melt (just below the boiling point) we expect that an appreciable number of As_4S_4 molecules will be present in the final products.

A brief survey on the Raman studies of As_4S_4 molecules embedded in various environments reveals the following facts. The As_4S_4 crystal (realgar) shows strong Raman peaks at 182, 192, 220, and 222 cm^{-1}.[17] Quite revealing are the data on the liquid state of pure As_4S_4 reported by Nemanich *et al.*,[18] where extra information on the polarization properties of vibrational modes were given. We note that the 186-cm^{-1} vibrational band is depolarized while the 221-cm^{-1} line is strongly polarized. This agrees with our finding mentioned above for the polarization properties of the corresponding bands of As_4S_4 molecules dispersed into the As_2S_3 glass structure. A Raman study of the irradiation-produced form of crystalline As_4S_4 called pararealgar,

TABLE I. Vibrational peak frequencies in cm^{-1} for an As_4S_4 molecule embedded in various environments. abbreviations and symbols are as follows. p: polarized, dp: depolarized, vw: very weak, vs: very strong, ↓: intensity decrease, ↓↓: strong intensity decrease, and X: peak absence from the spectrum.

Bulk glass and fiber[a]	Intensity change (heating)	Intensity change (light/stress)	As_4S_4 crystal[b]	As_4S_4 liquid[c]	pararealgar[d]
182 p	↓	↓	182		
189 dp	↓↓	↓↓	192	186 dp	191 vw
221 p	X	X	220, 222	221 p	
231 dp	↓↓	↓↓			230 vs
240 p	X	X			236 vs

[a]Present work. [c]Reference 18.
[b]Reference 17. [d]Reference 19.

p-As_4S_4, has been presented rather recently.[19] While both the realgar and pararealgar molecular units exhibit cagelike structures there are differences related to the intracage bonding arrangement. Indeed, as one can realize from Fig. 2(a) in the realgar arrangement each As atom forms two heteropolar As-S bonds and one homopolar As-As bond. In p-As_4S_4 there are three different bonding configurations, where the As atoms are bonded to one, two, or three S atoms. We close this discussion of the vibrational properties of As_4S_4 molecules by noting that elemental amorphous As, whose structure consists of pyramidal As_4 molecules, exhibits a strong broad Raman band which covers the spectral region 170–310 cm^{-1} and is centered at ~225 cm^{-1} (sputtered a-As) while a sharp feature at ~200 cm^{-1} is superimposed on this broad peak (bulk a-As).[20] The infrared spectrum of a-As shows a strong absorption band peaked at 230 cm^{-1}.[21]

It becomes evident from the above-mentioned details, which have also been compiled in Table I for convenience, that the vibrational peaks in spectral regions I and II originate from the vibrational modes of As_4S_4 arranged either in the realgarlike structure and/or in the pararealgar modification. There is a correspondence between the polarization properties of the 189- and the 221-cm^{-1} peaks in the glass (bulk and fiber) and the 186- and 221-cm^{-1} peaks in liquid As_4S_4, implying that they can be assigned to the As-As stretching and S-As-S bending modes, respectively, in As_4S_4 molecules. Quite interesting is the fact that modes of p-As_4S_4 are also evident in our data of the rapidly quenched bulk glass. This is asserted from the presence of the 231- and 240-cm^{-1} peaks in the latter. The analog of these peaks in p-As_4S_4 is the doublet located at 230 and 236 cm^{-1}, which has no counterpart in the Raman spectra of pure realgar.

B. An intramolecular structural mechanism for PiF

Based on the above arguments and on the diminishing of the 189- and 221-cm^{-1} bands of the optically processed fibers we can envisage the transformation of Figs. 2(a) →2(b)→2(c) as one of the possible structural mechanisms facilitating the photoinduced plastic changes. This transformation can be realized by the combined action of light and stress, which can untie As-As knots, resulting in an effective unfolding of the cagelike As_4S_4 molecule. The As atoms suspended at the ends of the As_4S_4 planar cluster are now amenable to bonding with S atoms. The latter are the excess S atoms needed to fulfill the stoichiometry of the As_2S_3 glass, which reside in the interstices of the structure. It is possible that the intermediate cluster with one broken As-As bond can be further modified and the linkage of the other two As atoms to network units might contribute to the substantial polymerization of the structure.

The proposed model is compatible with two key features of PiF. First, it can account for the length increase of the fiber through an opening of the ''closed'' As_4S_4 configuration. An attempt to quantitatively estimate the fractional length increase due to this model is presented below. Second, the specific atomic transformation engenders anisotropy through the transformation of a highly symmetric molecule to an asymmetric planarlike configuration, as is clearly evidenced in the depolarization ratio increase. These findings are important because they show that homopolar As-As bonds most likely dissociate rather than form during the time that photoplastic effects take place, a procedure that is reminiscent of that of thermal annealing.

C. A comparison between the kinetics of PiF and of Raman spectra changes

In what follows we try to elucidate the distinct role of intramolecular and intermolecular mechanisms by means of a comparison between the kinetics of photoinduced plastic deformation and the kinetics of changes of Raman spectra. Taking into account the lack of detailed information about the specific features of photoinduced plastic changes in chalcogenide glasses, we use here data concerning kinetics, i.e., the time dependence, of photoinduced fluidity, that has been studied by illuminating the glass using different laser power densities.[22] It should be stressed that though PiF can be induced with a range of laser power densities, in our studies we have used a power density of about ~30 $W\,cm^{-2}$. This is close to the lowest threshold value above which the effect was measurable and it was chosen in order to avoiding undesired sample heating. On the other hand, this low value of the power density renders the kinetics of the effect to be rather slow and this assures that fluidity can be considered essentially unchanged during the recording of a set of polarized and depolarized Raman spectra. Concerning the power-density dependence of PiF, it has been shown[22] that the photoinduced viscosity decreases by a factor of 8 when the power density on the glass varies from 20 to 100 $W\,cm^{-2}$. Further, the kinetics of PiF evidenced through the rate of increase of the elongation of the illuminated part of the glass also shows a monotonic, drastic increase when the laser power density increases gradually in the range 20–100 $W\,cm^{-2}$.[22]

Although quantitative conclusions regarding the kinetics of photoinduced fluidity and the kinetics of the changes observed in Raman spectra are not possible we proceed below to a comparison between the time dependence of the photoinduced elongation[22] of As_2S_3 glass and that of the magni-

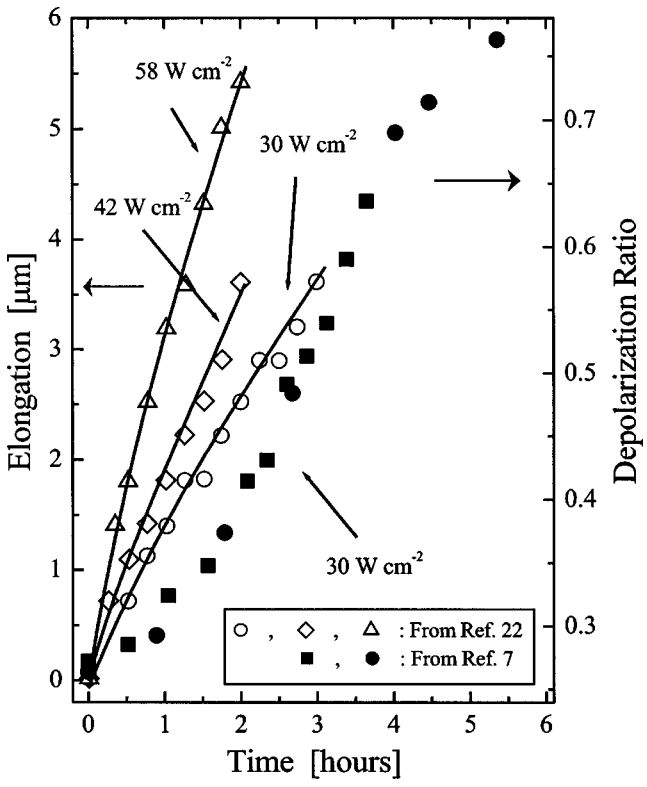

FIG. 3. Time dependence (kinetics) of (i) photoinduced As_2S_3 flake bending (open symbols, left-hand axis) and (ii) Raman spectra changes (solid symbols, right-hand axis).

tude of the depolarization ratio,[7,9] which accounts for the most significant changes observed in Raman spectra. We illustrate in Fig. 3 the kinetics of the As_2S_3 flake bending and the kinetics of the magnitude of the depolarization ratio of Raman spectra obtained from various fibers under elongational stress. Three data sets concerning the elongation of flake bending, which correspond to different laser power densities, i.e., 30, 42, and 58 $W\,cm^{-2}$, are presented. We observe that changes of Raman spectra, which correspond to $\sim$30 $W\,cm^{-2}$, exhibit a somewhat slower but analogous kinetics behavior compared to that of the flake bending. However, there is another important difference between the two experiments illustrated in Fig. 3. That is, while the bond ordering effects reflected by the depolarization ratio reach a saturation or plateau value, the elongation of flakes or fibers continues uninterruptedly, leading to fracture at long times for the latter. This implies that while the kinetics of Raman spectra changes can be normalized by the difference between the initial and final magnitudes of the depolarization ratio, no such normalization is possible for photoinduced elongation. The saturation of changes in Raman spectra after a certain time interval does not conflict with the fact that the ''flow'' process of the materials continues until the fracture limit. The saturation of the depolarization ratio implies that all mechanisms related to orientational changes and/or ordering effects cease to exist; defective structures (intramolecular and intermolecular) have been consumed and no appreciable structural changes can thus be detected by Raman scattering. The fact that the material continues to flow does not necessarily mean that there are other mechanisms of PiF in close analogy with stretching effects in polymers.

D. Quantitative estimation of the fractional intramolecular mechanism contribution to photoplastic changes

It would be instructive, despite some unavoidable speculation, to estimate the relative contribution of the intramolecular mechanism discussed in the present paper to the fiber elongation, in comparison to the elongation caused by intermolecular mechanisms such as layer unfolding. As has been already mentioned above, previous Raman data[16] have shown that the density of the homopolar bonds is of the order of $\sim$1% in the stoichiometric glass composition. In another approach to this issue,[23] the concentration of As_4S_4 molecules has been correlated to the position of the boson peak, which is a universal feature of amorphous solids and supercooled liquids situated at the low-frequency region of the Raman spectrum. According to this empirical correlation,[23] the position (frequency) of the boson peak is inversely proportional to the concentration of As_4S_4 units. In particular, when the frequency of the boson peak is located at $\sim$24 cm^{-1}, such as emerges in our case, the concentration of homopolar As-As bonds is of the order of 3% when the glass is obtained by quenching the liquid from 670 °C.

In a first approximation we consider that the proportion of As-As bonds, which are predominantly incorporated into S_2As-AsS_2 units,[18] is of the order of 2% (a mean value of the above estimations) compared to the energetically favorable As-S bonds. According to the model illustrated in Fig. 2, almost half of these homopolar bonds are destroyed during the transition of Figs. 2(a)$\rightarrow$2(b), which implies that the number of such bonds contributing to the plastic deformation of the fiber is $\sim$1% of the heteropolar As-S bonds. The other half of the As-As bonds, disrupted during the stage Figs. 2(b)$\rightarrow$2(c), can be viewed as offering structural relaxation in pathways other than that of the direction of the applied stress. As a consequence, and after adopting the reasonable assumption of a homogeneous distribution of the homopolar bonds in the glass structure, we expect that the distance between them is $\sim$10 Å given that the length of the As-S bond is $\sim$2.25 Å. A similar conclusion concerning the separation of As-As bonds has also been reached in Ref. 16. Using simple geometrical arguments, i.e., the values of the S-As-S angle ($\sim$95°) and the As-S distance, we find that the unfolding of the As_4S_4 molecule from configuration of Fig. 2(a) to 2(b) contributes a length increase of approximately 3 Å. However, for this estimation it has been assumed that after the breaking of the As-As bond the As atoms become coplanar with the four S atoms, which might not be necessarily true; therefore, a more realistic magnitude of the length increase during the opening of the As_4S_4 molecule is of the order of 2 Å. Given the above context, there is an increase of 2 Å over a region of 10 Å, which is the distance between defective configurations.

To facilitate the estimation of the fractional contribution of the intramolecular and intermolecular mechanisms let us denote by L the linear dimension of the illuminated part of the fiber, and ΔL the photoinduced elongation. ΔL is ex-

pected to arise from the summation of ΔL^{intra} and ΔL^{inter}, where the former denotes the contribution of the intramolecular and the latter of the intermolecular mechanisms. From the aforementioned arguments we expect that $\Delta L^{\text{intra}}/L \approx 0.2$. Based on our experimental results,[6–9] we have found that on the average the increase of the fiber's length is of the order of $\Delta L/L \approx 0.7$ at the time when ordering effects, evidenced through the magnitude of the depolarization ratio, reached a plateau value. Therefore, the fractional contribution of the intramolecular model as depicted in Fig. 2 can be estimated as $\Delta L^{\text{intra}}/\Delta L \approx 0.3$. Concluding, the above estimations yield that at room temperature almost 30% of the fiber's elongation comes from the unfolding of As_4S_4 molecules while the remaining 70% is associated with other intermolecular mechanisms such as layer flattening.[7,9,10] Finally, it should be stressed that the cagelike→planarlike mechanism advanced here as a possible source of PiF could also be employed to rationalize the well-known photoinduced volume expansion under sub-band-gap light illumination.[24] Indeed, in the absence of an external stimulus, such as an elongational stress, the As_4S_4 cage opening can contribute to a volume increase towards the direction of weaker constraints, that is, to a direction normal to the surface of a film. In particular, in the case of chalcogenide film irradiation—where photoinduced volume expansion is usually observed—films formed by evaporation contain an appreciably high fraction of As_4S_4 units and thus the structural mechanism model proposed in this paper becomes a likely model to explain the prominent photoinduced volume increase.

IV. CONCLUSIONS

Raman spectra of bulk glassy As_2S_3 at room and elevated temperatures (near T_g) and corresponding spectra of optically processed fibers under stress have been recorded and analyzed. Particular emphasis was placed on the intramolecular (bond-bending) region of the As_4S_4 molecular units. Reasons for the presence of such molecules in the stoichiometric glass structure have been discussed and the vibrational modes of As_4S_4 molecules in various environments have been compiled. It was thus shown that the experimental data are compatible with a microscopic picture which involves the transformation of cagelike As_4S_4 molecules into planarlike configurations amenable to polymerization within the network structure. The model has been suggested in view of the similarity between the spectra of the optically processed fiber and the annealed glass as well as in view of the fact that As_4S_4 molecules dissociate (annealing of As-As bonds) at temperatures near the glass transition temperature. It seems that wrong bonds may act as structural instabilities. This leads to a reduced ability of the structure to withstand plastic deformations and the glass network yields under the influence of the applied stress. This effect is analogous to the viscoplastic deformation of crystals under stress; an effect related to some instability due to the evolving dislocations.[25] In the case of PiF, the presence of wrong As-As bonds might be one of the possible factors destabilizing the glass structure. The proposed mechanism can as well serve as rationale for understanding the photoinduced volume expansion observed in chalcogenide glasses.

Kinetics of photoinduced plastic changes is compared to the kinetics of Raman spectra changes, and in particular with the time dependence of the depolarization ratio, revealing a qualitative similar behavior. An approximate estimation of the relative contribution of intermolecular processes, such as layer unfolding, and the intramolecular structural mechanism proposed in this paper has revealed that the latter is responsible for almost 30% of the photoinduced elongation of the fiber's length at room temperature. However, safer conclusions concerning the issues studied in the present paper await further experimental data due to the fact that photoinduced plastic changes have been tested only for a limited number of glasses. Finally, it is worth mentioning that PiF belongs to a general class of photoplastic changes observed in amorphous chalcogenides[11,26] that deserve further study since their origin is still at a speculative level.

*Electronic address: sny@iceht.forth.gr

[1] A. V. Kolobov and K. Tanaka, in *Handbook of Advanced Electronic and Photonic Materials and Devices, Chalcogenide Glasses and Sol-Gel Materials*, edited by H. S. Nalwa (Academic, New York, 2001), Vol. 5, pp. 47–90.

[2] K. Shimakawa, A. V. Kolobov, and S. R. Elliott, Adv. Phys. **44**, 475 (1995).

[3] H. Hisakuni and K. Tanaka, Science **270**, 974 (1995).

[4] G. N. Papatheodorou and S. N. Yannopoulos, in *Molten Salts: From Fundamentals to Applications*, edited by M. Gaune-Escard (Kluwer Academic, Dordrecht, 2002), pp. 47–106.

[5] S. R. Elliott, J. Non-Cryst. Solids **81**, 71 (1986).

[6] D. Th. Kastrissios, S. N. Yannopoulos, and G. N. Papatheodorou, Physica B **296**, 216 (2001).

[7] D. Th. Kastrissios, G. N. Papatheodorou, and S. N. Yannopoulos, Phys. Rev. B **64**, 214203 (2001).

[8] D. Th. Kastrissios and S. N. Yannopoulos, J. Non-Cryst. Solids **299–302**, 935 (2002).

[9] D. Th. Kastrissios, G. N. Papatheodorou, and S. N. Yannopoulos, Phys. Rev. B **65**, 165211 (2002).

[10] S. N. Yannopoulos, Phys. Lett. A **296**, 295 (2002).

[11] S. N. Yannopoulos, in *Photo-induced Metastability in Amorphous Semiconductors*, edited by A. V. Kolobov (Wiley-VCH, Berlin, 2003), pp. 119–137.

[12] A few remarks should be added here to prevent possible misinterpretations of the observed structural changes in fibers. One could argue that the fiber-drawing procedure from the melt might induce some ordering in the fiber, as has been earlier reported for As_2Se_3 [P. Hari, P. C. Taylor, W. A. King, and W. C. LaCourse, J. Non-Cryst. Solids **227–230**, 789 (1998), and references therein]. However, one has to emphasize the important differences in the fiber drawing between the present work and that of Hari *et al.* where fibers were pulled from the melt at a speed greater than 100 m/min. This procedure produced fibers with diameters of ~1 μm, while in our experiment much lower drawing rates (at least by one order of magnitude) are used,

leading to a fiber diameter $d \approx 100-300\ \mu$m. More importantly, Hari *et al.* found that the drawing-induced "crystallites" survived only at 77 K, and seemed to anneal to the amorphous phase at 300 K. In addition, our study showed that the depolarization ratios (quite sensitive to such ordering effects) of the unstressed fiber and the bulk glass were equal within experimental error. Therefore any traces of drawn-induced crystallization are not detectable and do not affect the results of the present work.

[13] P. J. S. Ewen and A. E. Owen, J. Non-Cryst. Solids **35–36**, 1191 (1980).
[14] M. Frumar, A. P. Firth, and A. E. Owen, Philos. Mag. B **50**, 463 (1984).
[15] Z. U. Borisova, *Glassy Semiconductors* (Plenum, New York, 1981).
[16] Ke. Tanaka, Phys. Rev. B **36**, 9746 (1987).
[17] R. Zallen and M. L. Slade, Phys. Rev. B **18**, 5775 (1978).
[18] R. J. Nemanich, G. A. N. Connell, T. M. Hayes, and R. A. Street, Phys. Rev. B **18**, 6900 (1978).
[19] M. Muniz-Miranda, G. Sbrana, P. Bonazzi, S. Menchetti, and G. Pratesi, Spectrochim. Acta, Part A **52**, 1391 (1996).
[20] J. S. Lannin, Phys. Rev. B **15**, 3836 (1977).
[21] G. Lucovsky and J. S. Knights, Phys. Rev. B **10**, 4324 (1974).
[22] Ke. Tanaka, C. R. Chimie **5**, 805 (2002).
[23] S. Mamedov, A. Kisliuk, and D. Quitmann, J. Mater. Sci. **33**, 41 (1998).
[24] H. Hisakuni and K. Tanaka, Appl. Phys. Lett. **65**, 2925 (1994).
[25] J. Li, K. J. Van Villet, T. Zhu, S. Yip, and S. Suresh, Nature (London) **418**, 307 (2002).
[26] M. L. Trunov, J. Non-Cryst. Solids **192–193**, 431 (1995), and references therein.